Dibenzyl disulfide adsorption on Cu(111) surface: a DFT study

Mario Saavedra-Torres, Frederik Tielens, Juan C. Santos

Dibenzyl Disulfide Adsorption on Cu(111) Surface: A DFT Study

Mario Saavedra-Torres[1], Frederik Tielens[2,*], Juan C. Santos[1,*]

[1]Departamento de Ciencias Químicas, Facultad de ciencias exactas, Universidad Andres Bello, Av. República 275, Santiago, Chile.

[2]UPMC Univ. Paris 06, UMR 7574, Laboratoire Chimie de la Matière Condensée, Collège de France, 11 place Marcelin Berthelot, 75231 Paris Cedex 05, France.

Abstract

The adsorption of dibenzyl disulfide (*DBDS*) on a Cu(111) surface model was investigated by using density functional (DFT) calculations, considering energetic and electronic aspects. Several complexes were generated, where the bridge, hollow hcp, hollow fcc and top adsorption sites were considered. The results show that the Cu-S interaction guides the final complexes, and a secondary π-Cu weak interaction confers an extra stability. The complexes were grouped as physi- or chemi-sorption according to their adsorption energy applying a distortion decomposition model, with a preference by a double interaction of S with Cu (i.e. hollow hcp, and bridge sites). A degree of disulfide bond dissociation was observed in the complexes, being correlated with adsorption energies. From an electronic aspect, it was found that the electronic flow from copper to *DBDS* occurs in the most stables complexes, checked with charge analysis. These results are agreed with experimental revelations of copper corrosion on power transformers.

Keywords: Copper, dibenzyl disulfide (DBDS), DFT, adsorption

---

[*]Corresponding authors:
Juan Carlos Santos: jsantos@unab.cl
Frederik Tielens: frederik.tielens@upmc.fr

Introduction

The adsorption of sulfur containing molecules on gold surfaces have attracted much attention and this especially since the discovery of the self-assembly of alkyl thiols on Au(111).[1-3] Thiols adsorption has also been studied on the other coinage metals[4-7]. Thiols[4, 8-15], disulfides[16-19], methionines[20-24], cysteines[25-33], etc. have been studied experimentally and theoretically. The reactivity towards sulfur containing molecules decreases going down the column of the coinage metals, explaining why molecular adsorption has been successfully observed in the perfectly ordered thiol chains on Au(111) (See reviews on the topic cited higher). On Cu(111), the more reactive surface of the three metals (Cu, Ag, Au), a different picture of the adsorption is expected and observed[5, 34, 35]. The surface itself will reconstruct and the adsorbed molecules easily dissociated.

Thus, understanding the mechanism of interaction of sulfur containing molecules is expected to be of high relevance for opening new perspectives towards improving the reactivity or stability of materials used in different applications[36]. Concerning the copper surfaces, sulfur containing molecules induce copper metal corrosion, which is a chemical phenomenon that triggers serious failures in industrial applications, and especially in power transformers[37, 38].

Dibenzyl disulfide (*DBDS*) is an additive with antioxidant properties, frequently used in insulating mineral oil employed in power transformers. Under operation conditions, *DBDS* is known to further copper corrosion in electric equipment, by forming copper (I) sulfide Cu_2S as the main product, with the subsequent production of other sulfur compounds such as benzyl sulfide and dibenzyl sulphide. In spite of successive studies about the chemical phenomenon, the mechanism remains unclear[39-42]. Since *DBDS* is related to the commonly used thiol molecules, in the well-known thiol self-assembled monolayers (SAM) on metal surfaces, [9, 43-45], the analysis of the metal-sulfur bond is important to complete the already known information on the chemical properties of this type of systems.

In the present paper, the nature of the interaction between Cu(111) and *DBDS* is theoretically studied. A slab model is used to simulate the copper surface at reasonable accuracy, i.e. using periodic PBE-D2. In particular we clarify some aspects associated with copper corrosion by *DBDS* at the DFT level by accounting geometric, energetic and electronic properties that govern the interaction between *DBDS* and copper. The main focus of attention is to characterize locally the copper-sulfur interaction/bonding.

Computational Details

1. Computational Method

Calculations were performed in the frame of periodic DFT by means of the Vienna Ab Initio Simulation Package (VASP 5.3).[46,47] The electron-ion interactions were described by the projector augmented wave (PAW) method [48, 49], representing the valence electrons. The convergence of the plane-wave expansion was obtained with a cut-off of 400 eV. The Perdew-Burke-Ernzerhof (PBE)[50,51], a Generalized Gradient Approximation (GGA) functional was used. The adsorption of *DBDS* (See Fig. 1) on Cu(111) was modeled using a c7×7 periodic unit cell, with the aim to the study the adsorption of an isolated adsorbate molecule interacting with the surface. The Cu slab contains three layers, from which the bottom one was not allowed to relax and kept at the bulk positions. The lattice parameter was initially fixed at the experimental value, 3.61 Å, to build the initial slab[52]. Then, it was re-optimized and a subestimation of 3% from the original supercell was obtained. This small change is accepted because is in good agreement with the experimental parameter and the obtained theoretically from PBE[53].

The sampling in the Brillouin zone was performed employing 4 and 13 k-points, resolved on 2×2×1 and 5×5×1 grids for the geometry optimizations (including dispersion corrections) and energy evaluation (at single PBE level), respectively.

Since our system involved organic molecules interacting through weak forces, the pure DFT energies obtained in periodic DFT PBE should be corrected. Therefore, we included Grimme D2 corrections[54], which can be calculated using the presently used VASP version, although, D2 corrections overestimate the binding energy ([55, 56] and references therein).
The optimization procedure consisted of locate initially the *DBDS* molecule at 2.3 Å from the surface, at the beginning of the geometry relaxation. This distance was taken from chemi- and physisorption data reported in several studies involving the adsorption of sulfur molecules on copper surfaces[34, 35, 57, 58].

2. Calculation of the adsorption energy and charge transfer

Each complex can be characterized by its adsorption energy, ΔE_{ads}, which is calculated from the total energy of the ground state optimized geometries of the complex, Cu(111) slab and *DBDS* as following:

$$\Delta E_{ads} = E_{Cu(111)\text{-}DBDS} - [\ E_{Cu(111)} + E_{(DBDS)}\ ] \tag{1}$$

$$\Delta E_{ads.D2} = \Delta E_{ads} + [\ E_{Cu(111)\text{-}DBDS.D2} - [\ E_{Cu(111).D2} + E_{(DBDS).D2}\ ]\ ] \tag{2}$$

Eq (2) includes the dispersion contribution D2, explicitly for each term.
However, this term can be scaled to obtain a better energetic estimation, avoiding the most part of the overestimation of empirical of the metal bulk. A common used correction is that the adsorption energy is approximated to include only the dispersion from the top layer of the surface and the adsorbate (*DBDS*), defining the term $\Delta E_{ads.D2.1layer}$ as:

$$\Delta E_{ads.D2.1layer} = \Delta E_{ads} + [\ \frac{1}{3}(E_{Cu(111)\text{-}DBDS.D2}\ ) - [\ \frac{1}{3}E_{Cu(111).D2} + E_{(DBDS).D2}] \tag{3}$$

Moreover, an energetic decomposition scheme can be inspected, to describe energetically the change along the adsorption process, through a two part scheme of deformation/interaction[59]. This partition scheme consists of two contributions, deformation (ΔE_{def}), and interaction energy (ΔE_{int}), related as:

$$\Delta E_{ads} = \Delta E_{def} + \Delta E_{int} \tag{4}$$

Where

$$\Delta E_{def}(\ X\ ) = E(X_{deformed}) - E(X_{equilibrium}) \quad ; X = Cu_{(111)}, DBDS \tag{5}$$

ΔE_{def} precise an energetic measure of perturbation over the gas phase equilibrium geometry of each molecule, to obtain their respective geometry in the complex. Is clear, that $\Delta E_{int,}$ represents the interaction energy between the deformed molecules in the complex and can be easily computed, from eq. (4) and (5).

4

The amount of total electronic charge transferred between *DBDS* and the Cu surface, was quantified by a Global Charge Transfer descriptor (*GCT*), which corresponds to the sum of atomic charges (q_A) on each molecule (A), i.e. the *DBDS* or the surface:

$$GCT = \sum_A q_A \quad ; \quad A \in Cu_{surf} \text{ or } DBDS \tag{6}$$

For this purpose the Bader Charge Analysis[60, 61] was used.

Additionally, the Electron Localization Function (ELF) was studied to characterize the existence of the S-S bond while the *DBDS* interact with the surface. The ELF of Becke and Edgecombe [62] provides an orbital independent description of the electron localization based on strong physical arguments regarding the Fermi hole. The ELF is defined in terms of the excess of local kinetic energy density due to the Pauli Exclusion Principle and the Thomas-Fermi kinetic energy density. Its numerical values are conveniently mapped on the interval (0,1) facilitating its analysis. According to the interpretation of the ELF, a region of the space with a high value of ELF corresponds to a region where it is more probable to localize a pair of electrons of opposite spin. The topological analysis of the ELF gradient field [63-65] provides a mathematical model enabling the partition of the molecular position space in a set of continuous and non-overlapping basins of attractors that present in principle a one-to-one correspondence with electron pairs.

In this way, an accurate calculation of chemical local objects such as bonds, lone pairs, or atomic shells can be achieved. The basins are either core basins labeled C(A) or valence basins V(A,...) belonging to the outermost shell. Valence basins are characterized by their coordination number (synaptic order) with core [66]. The original work of Silvi and Savin on the ELF generated a fruitful field of applications in a variety of chemical problems, ranging from structural and chemical reactivity studies as well as the study of chemical reactions[67-70]. This scheme will be applied to evaluate the S-S bond in the complex.

Results and discussion

Geometric and Energetic Aspects

In this work, 20 optimized adsorption complexes were defined combining the different possible S adsorption sites on Cu(111) surface (top, hollow hcp, hollow fcc, and bridge) with the three iso-energetic *DBDS* gas phase conformations, obtained from a previous study[71] (See **Fig. 1**).

Using PBE, the structure B was more stable than A and C conformers by 0.03 and 0.07 eV respectively. It confirms the isoenergetic character of three conformers. In the succeeding optimization procedures, the adsorption complexes between *DBDS* and Cu(111) results with different interaction sites, mainly noticed by S-Cu geometrical parameters. A schematic representation of showing selected geometrical parameters is presented in **Fig 2**.

Typically, the adsorption site for both S atoms is found close to a bridge site. Other adsorption sites slightly higher in energy are also present, such as on top (close). Different adsorption geometries (mainly due to different benzyl conformations) showing different adsorption energies can adsorb on the same adsorption site. In order to rationalize the data, we defined the vertical spacing distance Δz and the shortest S-Cu distance, d1 and d2 (See **Fig. 2, Table 1**).

The most stable physisorbed geometries, shown in **Fig. 3**, can be divided in two groups: a) having an S-Cu atop adsorption and b) 2S-Cu atop adsorption. The first is slightly more favorable (structure B7). It should be noted that the benzyl groups tend to orient parallel to the Cu(111) surface.

From Table 1, the S-S distances (d3) between 2.0 and 2.2 Å, corresponds to physisorbed complexes and also correlates with a high average values of d1 and d2 (> 2.56 Å), with adsorption sites that vary between bridge, top and hollow sites. In the other side, the group of structures having d3 distance larger than 3.4 Å and an average of d1 and d2 lower than 2.56 describes the chemisorption complexes, where sulfur atom prefers the adsorption on bridge (slightly to hollow) sites.

In summary the most favorable adsorption sites was found to be bi-coordinated bridge in the case of physisorption and a bridge (slightly to hollow) for each dissociated fragment of benzylthiol, in the case of chemisorption (**See Fig. 3 and Fig. 5**).

The Δz distance is related to the strength of the interaction of the sulfur atom with the Cu(111) surface. Moreover, the difference of the vertical spacing between the S atom and the closest Cu surface atom and Δz give a geometrical measure for the deformation of the surface. After adsorption, and especially with dissociative chemisorption, a Cu atom can be lifted up out of the surface, and can be considered as a precursor state to the formation of an adatom. Similar results have been reported in the adsorption of thiols on Au and Ag surfaces, being less evident than Cu, attributable to the metal hardness. Looking at Δz in **Table 1**, one can conclude that the effect of chemisorption on the z coordinate of the surface copper atoms is particularly noticeable over $\Delta z1$, where values of $\Delta z1$ lower than 5.98 corresponds to chemisorbed species, while higher than this value are related with physisorption complexes. The most affected copper atoms of the top layer, are lifted up by 0.2 Å. The magnitude of surface deformation due to the tension generated by the adsorption of *DBDS* will certainly increase with increasing coverage, as is noticed in thiol/Au(111) SAMs.[9, 72] This surface tension is observed over a range of copper atoms in the neighborhood of the binding sulfur atom (See **Fig. 4**).

The adsorption energies (See **Table 2**) are in agreement with the geometrical parameters. Indeed the adsorption complexes having the shortest distances between the *DBDS* sulfur atom and the Cu(111) surface (d1,d2), correlates with the highest (absolute value) adsorption energies. The adsorption energy helps to identify that the phenyl-Cu proximity, shows a weak π-Cu interaction (see lower), leads to an extra stabilization of the adsorption complexes (structures B1, B2, and B3), which correspond to the chemisorbed species (See **Fig. 5**).

In general the complexes formed from conformer type B and C (See **Fig. 1**), have more stable adsorption energies due to the proximity of the phenyl groups to the surface, favoring π-Cu interactions.

The deformation/interaction decomposition scheme displayed in **Table 3**, shows that in case of physisorbed complexes, the surface is slightly more perturbed than *DBDS*. The low values of ΔE_{def} and almost the total contribution of ΔE_{int} to ΔE_{ads}, explain the low geometrical effect in the

adsorption. In the other side for chemisorbed complexes, the ΔE_{def} are higher and particularly $\Delta E_{def}(DBDS)$ is greater than the surface and it represents more than 70% of ΔE_{ads} with the inclusion of an important part of the dissociative process. Additionally, $\Delta E_{def}(DBDS)$ represents more than the 50% of absolute value of ΔE_{int}, while the ΔE_{def} (Cu) is less than 5% for ΔE_{int}. Those assesses, explains an important role of the geometry relaxation of *DBDS* related with dissociation over the adsorption.

Electronic Aspects:

Global Charge Transfer

A global charge transfer descriptor was introduced to quantify the relation between the adsorption energies and charge transfer between *DBDS* and the Cu(111) surface. **Table 2** summarizes this quantity. It can be seen that the direction of the charge transfer is highly related to the kind of adsorption (physi- or chemi-sorption). In the most stable cases (B1, B2, and B3, i.e. chemisorbed species), the *DBDS* molecule acts as an electron acceptor. Most transferred charge is then allocated on the disulfide group, reaching a maximum when dissociation of the S-S bond occurs. Conversely, in the physisorption processes the *DBDS* molecule act as donor but with a lower rate of charge transfer to the Cu(111) surface (See **Fig. 6**).

Also, a spontaneous (barrier less) dissociation of the disulfide bond is observed for chemisorbed species, which increases the ability of *DBDS* to become an electron acceptor. In this case, the S-S distance increases from 2.0 to 2.2 Å and from 3.5 to 4.5 Å for physisorption and chemisorption, respectively. Finally, bi-coordinated interactions of the sulfur atoms with the Cu atoms and preferential orientation of the phenyl rings parallel to the Copper surface were observed.

Electron Localization Function (ELF) Analysis.

In the **Fig 7** a representation of the ELF basins is shown to help visualize the most relevant regions of valence electron density that characterize the *DBDS* in its adsorption process on copper surface.

The basin population analysis using pseudopotentials is not accurate enough, mainly to describe the population associate to sulfur atoms. However, the topological description gives us important information about the bonds in the different obtained complexes in this work.

In all kind of formed complexes by physi- or chemi-sorption, each benzylsulfide moiety of the adsorbed *DBDS* presents two kinds of C-H bonds, aromatic (6) and methylene (2), represented by disynaptic basins V(H,C). The six carbon-carbon aromatic bonds are represented by disynaptic V(C-C), the shape and inclusive, the population close to 3e is characteristic of delocalized bond in aromatic systems, and the one non aromatic bond, V(C-C), has population close to 2.1 e. Around the sulfur atom is possible to visualize the disynaptic V(C-S) with population between 1-1.5e and two monosynaptic basins V(S) which characterize the electron lone pairs. At least, one of this are located between sulfur and surface. But the main difference are centered in the disynaptic basin V(S-S), which describes the disulfide bond. In the physisorption complexes is possible to visualize it but in the chemisorption complexes this basin disappears. It indicates the disulfide dissociation in the most stable formed complexes.

Corroboration of topological description was made using the structure of isolated *DBDS* with the geometry adopted in the complex. First at the same level of calculation previously described and confirmed by all electron calculation using the same functional and def2-TZVP basis set. The same description was obtained, and the disynaptic V(S-S) appears and disappears in the *DBDS* physi- and chemi-sorption complexes, respectively.

Conclusions

The molecular (physisorption) and dissociative (chemisorption) adsorption of *DBDS* on Cu(111) was studied by means of periodic DFT. Physisorption was investigated in detail by optimizing systematically all possible conformations. The adsorption site was found to be bi-coordinated bridge for physisorption and on simple bridge for chemisorption. The adsorption energies were calculated and decomposed, validating the high contribution of relaxation in the adsorption process. The charge transfer and the ELF function were used to describe the electronic structure of the adsorption complex. It was found that a charge transfer from the Cu(111) surface to the disulfide group occurs, reaching a maximum in the structures where S-S bond dissociation is observed, whereas in the physisorption processes the *DBDS* molecule act as donor but with a lower rate of charge transfer to the Cu surface. The ELF shows the absence and presence of the S-S bond in chemisorption and physisorption, respectively.

The dissociative adsorption of *DBDS* on Cu(111) can be considered as the first step of the copper corrosion phenomenon in which an oxidation process takes place on the surface.

References

1.   A. Ulman, *Chemical Reviews*, 1996, **96**, 1533-1554.
2.   J. C. Love, L. A. Estroff, J. K. Kriebel, R. G. Nuzzo and G. M. Whitesides, *Chemical Reviews*, 2005, **105**, 1103-1169.
3.   C. Vericat, M. E. Vela, G. Benitez, P. Carro and R. C. Salvarezza, *Chemical Society Reviews*, 2010, **39**, 1805-1834.
4.   F. P. Cometto, P. Paredes-Olivera, V. A. Macagno and E. M. Patrito, *The Journal of Physical Chemistry B*, 2005, **109**, 21737-21748.
5.   H. Gronbeck, *The Journal of Physical Chemistry C*, 2010, **114**, 15973-15978.
6.   P. E. Laibinis, G. M. Whitesides, D. L. Allara, Y. T. Tao, A. N. Parikh and R. G. Nuzzo, *Journal of the American Chemical Society*, 1991, **113**, 7152-7167.
7.   K. A. Kacprzak, O. Lopez-Acevedo, H. Hakkinen and H. Gronbeck, *The Journal of Physical Chemistry C*, 2010, **114**, 13571-13576.
8.   M. H. Fonticelli, G. Benitez, P. Carro, O. Azzaroni, R. C. Salvarezza, S. Gonzalez, D. Torres and F. Illas, *The Journal of Physical Chemistry C*, 2008, **112**, 4557-4563.
9.   N. B. Luque, E. Santos, J. Andres and F. Tielens, *Langmuir*, 2011, **27**, 14514-14521.
10.   T. Sawaguchi, Y. Sato and F. Mizutani, *Journal of Electroanalytical Chemistry*, 2001, **496**, 50-60.
11.   D. P. Woodruff, *Applied Surface Science*, 2007, **254**, 76-81.
12.   D. P. Woodruff, *Physical Chemistry Chemical Physics*, 2008, **10**, 7211-7221.
13.   F. Tielens, D. Costa, V. Humblot and C. M. Pradier, *The Journal of Physical Chemistry C*, 2008, **112**, 182-190.
14.   F. Tielens and E. Santos, *The Journal of Physical Chemistry C*, 2010, **114**, 9444-9452.
15.   T. Doneux, F. Tielens, P. Geerlings and C. Buess-Herman, *The Journal of Physical Chemistry A*, 2006, **110**, 11346-11352.
16.   W. Andreoni, A. Curioni and H. Gronbeck, *International Journal of Quantum Chemistry*, 2000, **80**, 598-608.
17.   F. P. Cometto, V. A. Macagno, P. Paredes-Olivera, E. M. Patrito, H. Ascolani and G. Zampieri, *The Journal of Physical Chemistry C*, 2010, **114**, 10183-10194.
18.   R. Di Felice and A. Selloni, *The Journal of Chemical Physics*, 2004, **120**, 4906-4914.
19.   H. Gronbeck, A. Curioni and W. Andreoni, *Journal of the American Chemical Society*, 2000, **122**, 3839-3842.
20.   V. Humblot, F. Tielens, N. B. Luque, H. Hampartsoumian, C. Methivier and C.-M. Pradier, *Langmuir*, 2014, **30**, 203-212.
21.   A. Naitabdi and V. Humblot, *Applied Physics Letters*, 2010, **97**.
22.   C. Méthivier, V. Humblot and C.-M. Pradier, *Surface Science*, 2015, **632**, 88-92.
23.   A. Schiffrin, A. Riemann, W. Auwarter, Y. Pennec, A. Weber-Bargioni, D. Cvetko, A. Cossaro, A. Morgante and J. V. Barth, *Proceedings of the National Academy of Sciences of the United States of America*, 2007, **104**, 5279-5284.
24.   A. Schiffrin, J. Reichert, Y. Pennec, W. Auwaerter, A. Weber-Bargioni, M. Marschall, M. Dell'Angela, D. Cvetko, G. Bavdek, A. Cossaro, A. Morgante and J. V. Barth, *The Journal of Physical Chemistry C*, 2009, **113**, 12101-12108.
25.   V. De Renzi, L. Lavagnino, V. Corradini, R. Biagi, M. Canepa and U. del Pennino, *The Journal of Physical Chemistry C*, 2008, **112**, 14439-14445.

26. R. Di Felice, A. Selloni and E. Molinari, *The Journal of Physical Chemistry B*, 2003, **107**, 1151-1156.
27. G. Gonella, S. Terreni, D. Cvetko, A. Cossaro, L. Mattera, O. Cavalleri, R. Rolandi, A. Morgante, L. Floreano and M. Canepa, *The Journal of Physical Chemistry B*, 2005, **109**, 18003-18009.
28. B. Hoffling, F. Ortmann, K. Hannewald and F. Bechstedt, *Adsorption of Cysteine on the Au(110)-surface: A Density Functional Theory Study*, Springer-Verlag Berlin, Berlin, 2010.
29. S. Fischer, A. C. Papageorgiou, M. Marschall, J. Reichert, K. Diller, F. Klappenberger, F. Allegretti, A. Nefedov, C. Woell and J. V. Barth, *The Journal of Physical Chemistry C*, 2012, **116**, 20356-20362.
30. N. B. Luque and E. Santos, *Langmuir*, 2012, **28**, 11472-11480.
31. E. Santos, L. Avalle, K. Poetting, P. Velez and H. Jones, *Electrochimica Acta*, 2008, **53**, 6807-6817.
32. E. Santos, L. B. Avalle, R. Scurtu and H. Jones, *Chemical Physics*, 2007, **342**, 236-244.
33. E. M. Marti, C. Methivier and C. M. Pradier, *Langmuir*, 2004, **20**, 10223-10230.
34. H. Rieley, G. K. Kendall, A. Chan, R. G. Jones, J. Lüdecke, D. P. Woodruff and B. C. C. Cowie, *Surface Science*, 1997, **392**, 143-152.
35. X.-L. Fan, Y. Liu, R.-X. Ran and W.-M. Lau, *The Journal of Physical Chemistry C*, 2013, **117**, 6587-6593.
36. S. M. Barlow and R. Raval, *Surface Science Reports*, 2003, **50**, 201-341.
37. V. Tumiatti, R. Maina, F. Scatiggio, M. Pompili and R. Bartnikas, *Conference Record of the 2008 IEEE International Symposium on Electrical Insulation*, 2008, 284-286.
38. J. M. Lukic, S. B. Milosavljevic and A. M. Orlovic, *Industrial and Engineering Chemistry Research*, 2010, **49**, 9600-9608.
39. S. Toyama, J. Tanimura, N. Yamada, E. Nagao and T. Amimoto, *IEEE Transactions on Dielectrics and Electrical Insulation*, 2009, **16**, 509-515.
40. F. Ahmed Khan, J. Sundara Rajan, M. Z. a. Ansari and S. Asra P, *2012 International Conference on Advances in Power Conversion and Energy Technologies (APCET)*, 2012, 1-4.
41. G. a. Oweimreen, a. M. Y. Jaber, a. M. Abulkibash and N. a. Mehanna, *IEEE Transactions on Dielectrics and Electrical Insulation*, 2012, **19**, 1962-1970.
42. R. Maina, V. Tumiatti, M. Pompili and R. Bartnikas, *IEEE Transactions on Dielectrics and Electrical Insulation*, 2009, **16**, 1655-1663.
43. F. Tielens, V. Humblot and C.-M. Pradier, *International Journal of Quantum Chemistry*, 2008, **108**, 1792-1795.
44. F. Tielens, V. Humblot, C. M. Pradier, M. Calatayud and F. Illas, *Langmuir*, 2009, **25**, 9980-9985.
45. F. Tielens and E. Santos, *The Journal of Physical Chemistry C*, 2010, **114**, 9444-9452.
46. G. Kresse and J. Hafner, *Physical Review B*, 1993, **47**, 558-561.
47. G. Kresse and J. Hafner, *Physical Review B*, 1994, **49**, 14251-14269.
48. P. E. Blochl, *Physical Review B*, 1994, **50**, 17953-17979.
49. G. Kresse and D. Joubert, *Physical Review B*, 1999, **59**, 1758-1775.
50. B. Hammer, L. B. Hansen and J. K. Norskov, *Physical Review B*, 1999, **59**, 7413-7421.
51. J. P. Perdew, K. Burke and M. Ernzerhof, *Physical Review Letters*, 1997, **78**, 1396-1396.
52. M. E. Straumanis and L. S. Yu, *Acta Crystallographica Section A*, 1969, **25**, 676-682.
53. C. Gattinoni and A. Michaelides, *Faraday Discuss*, 2015, **180**, 439-458.

54. S. Grimme, *Journal of Computational Chemistry*, 2006, **27**, 1787-1799.
55. N. Almora-Barrios, G. Carchini, P. Blonski and N. Lopez, *Journal of Chemical Theory and Computation*, 2014, **10**, 5002-5009.
56. J. Klimes and A. Michaelides, *The Journal of Chemical Physics*, 2012, **137**, 120901.
57. a. Ferral, E. M. Patrito and P. Paredes-Olivera, *The Journal of Physical Chemistry B*, 2006, **110**, 17050-17062.
58. E. R. Crutcher, K. Warner and M. Northwest, *electric-connectionco.com*.
59. J. Scaranto, G. Mallia and N. M. Harrison, *Computational Materials Science*, 2011, **50**, 2080-2086.
60. G. Henkelman, A. Arnaldsson and H. Jónsson, *Computational Materials Science*, 2006, **36**, 354-360.
61. W. Tang, E. Sanville and G. Henkelman, *Journal of Physics: Condensed Matter*, 2009, **21**, 084204.
62. A. D. Becke and K. E. Edgecombe, *The Journal of Chemical Physics*, 1990, **92**, 5397.
63. A. Savin, A. D. Becke, J. Flad, R. Nesper, H. Preuss and H. G. von Schnering, *Angewandte Chemie International Edition in English*, 1991, **30**, 409-412.
64. A. Savin, O. Jepsen, J. Flad, O. K. Andersen, H. Preuss and H. G. von Schnering, *Angewandte Chemie International Edition in English*, 1992, **31**, 187-188.
65. B. Silvi and A. Savin, *Nature*, 1994, **371**, 683-686.
66. B. Silvi, *Journal of Molecular Structure*, 2002, **614**, 3-10.
67. J. Melin and P. Fuentealba, *International Journal of Quantum Chemistry*, 2003, **92**, 381-390.
68. P. Fuentealba, E. Chamorro and J. C. Santos, 2007, vol. 19, pp. 57-85.
69. J. C. Santos, J. Andres, A. Aizman, P. Fuentealba and V. Polo, *The Journal of Physical Chemistry A*, 2005, **109**, 3687-3693.
70. J. C. Santos, W. Tiznado, R. Contreras and P. Fuentealba, *The Journal of Chemical Physics*, 2004, **120**, 1670-1673.
71 M. Saavedra-Torres, P. Jaque, F. Tielens and J. C. Santos, *Theoretical Chemistry Accounts*, 2015, **134**, 73.
72. E. Bedford, V. Humblot, C. Méthivier, C. M. Pradier, F. Gu, F. Tielens and S. Boujday, *Chem. Eur.* 2015, **21**, 14555-14561.

Table 1. Geometrical parameters describing the final adsorption geometries and sites: d1, d2, d3 and Δz (for sulfur 1 and sulfur 2, See **Fig. 2**). (values in Å).

Complex	Final Adsorption Site (S1 S2)		d1	d2	d3	$\Delta z1$	$\Delta z2$
A1	bridge-top	bridge-top	2.75	2.98	2.09	6.47	6.29
A2	bridge-top	bridge-top	2.78	2.66	2.09	6.19	6.28
A3	top	top	2.96	2.99	2.09	6.48	6.39
A4	bridge-top	bridge-top	2.97	3.02	2.09	6.51	6.42
A5	hollow1-top	bridge-top	2.57	2.87	2.11	6.51	6.13
A6	hollow1-top	bridge-top	2.56	2.95	2.14	6.48	6.07
A7	bridge-top	bridge	2.87	3.06	2.08	6.71	6.42
B1	hollow1-bridge	hollow1-bridge	2.41	2.42	4.42	5.98	5.96
B2	hollow1-bridge	hollow1	2.49	2.31	3.42	5.81	6.03
B3	hollow1-top	hollow2	2.81	2.24	3.92	5.67	6.30
B4	top	bridge-top	2.93	2.85	2.09	6.38	6.37
B5	bridge-top	bridge-top	2.66	2.70	2.13	6.24	6.18
B6	top	top	3.00	3.04	2.08	6.58	6.36
B7	top	bridge-top	2.82	2.95	2.10	6.40	6.30
B8	hollow2-top	hollow1-top	3.02	2.92	2.07	6.58	6.69
C1	top	top	2.96	2.97	2.10	6.37	6.46
C2	hollow2-bridge	hollow1-bridge	2.58	2.61	2.18	6.14	6.09
C3	top	bridge-top	2.95	2.76	2.09	6.29	6.43
C4	hollow1-top	hollow2-top	2.77	2.77	2.15	6.40	6.42
C5	hollow2-top	hollow1	3.00	3.05	2.07	6.76	6.65

Table 2. Adsorption energy (ΔE_{ads}) and sum of charges (q) on the Cu(111) surface and disulfide S-S atoms in the complexes investigated. (Values in eV, charges in e)

Complex	$\Delta E_{ads.D2.all}$	$\Delta E_{ads.PBE}$	$\Delta E_{ads.D2.1layer}$	$q_{Cu(111)}$	$q_{(S-S)}$
A1	-2.09	-0.40	-0.54	-0.14	0.02
A2	-2.03	-0.19	-0.38	-0.10	-0.04
A3	-2.03	-0.52	-0.60	-0.17	0.02
A4	-2.01	-0.58	-0.63	-0.14	0.01
A5	-1.94	-0.25	-0.39	-0.10	-0.02
A6	-1.87	-0.26	-0.38	-0.08	-0.06
A7	-1.54	-0.22	-0.23	-0.11	-0.02
B1	-3.84	-1.18	-1.67	0.67	-0.76
B2	-3.76	-1.01	-1.53	0.67	-0.77
B3	-3.48	-1.03	-1.45	0.62	-0.72
B4	-2.57	-0.21	-0.60	-0.08	-0.05
B5	-2.52	0.07	-0.40	0.01	-0.13
B6	-2.51	0.12	-0.36	-0.09	-0.06
B7	-2.50	-0.14	-0.53	-0.09	-0.05
B8	-1.89	0.10	-0.16	-0.08	-0.05
C1	-2.76	0.17	-0.43	-0.12	0.02
C2	-2.52	0.18	-0.34	0.05	-0.16
C3	-2.34	-0.23	-0.55	-0.10	0.00
C4	-1.98	-0.12	-0.36	-0.03	-0.07
C5	-1.82	-0.09	-0.28	-0.08	-0.02

Table 3. Deformation energies (ΔE_{def}) of surface and *DBDS*, and interaction energies (ΔE_{int}) for complexes, in presence and absence of D2 vdW contribution (in eV). Chemisorption complexes are highlighted.

Complex	$\Delta E_{def}(Cu)$	$\Delta E_{def}(DBDS)$	$\Delta E_{def}(Cu+DBDS)$	ΔE_{intD2}	ΔE_{int}
A1	0.15	0.07	0.22	-2.31	-0.66
A2	0.15	0.06	0.21	-2.24	-0.50
A3	0.11	0.11	0.22	-2.25	-0.67
A4	0.15	0.02	0.17	-2.19	-0.69
A5	0.17	0.11	0.28	-2.22	-0.57
A6	0.18	0.09	0.27	-2.15	-0.56
A7	0.14	0.04	0.18	-1.72	-0.36
B1	0.21	3.64	3.85	-7.69	-5.02
B2	0.28	3.13	3.41	-7.17	-4.39
B3	0.35	3.45	3.80	-7.28	-4.68
B4	0.15	0.20	0.35	-2.92	-0.48
B5	0.18	0.27	0.45	-2.97	-0.29
B6	0.17	0.26	0.43	-2.94	-0.24
B7	0.14	0.18	0.33	-2.82	-0.40
B8	0.08	0.10	0.18	-2.07	-0.03
C1	0.15	0.31	0.46	-3.21	-0.32
C2	0.17	0.31	0.48	-3.00	-0.33
C3	0.14	0.16	0.30	-2.63	-0.52
C4	0.20	0.09	0.29	-2.27	-0.34
C5	0.08	0.04	0.12	-1.95	-0.18

Figures

Fig 1. Three DBDS conformers of lowest energy used in this study as starting structure to generate the adsorption complex.
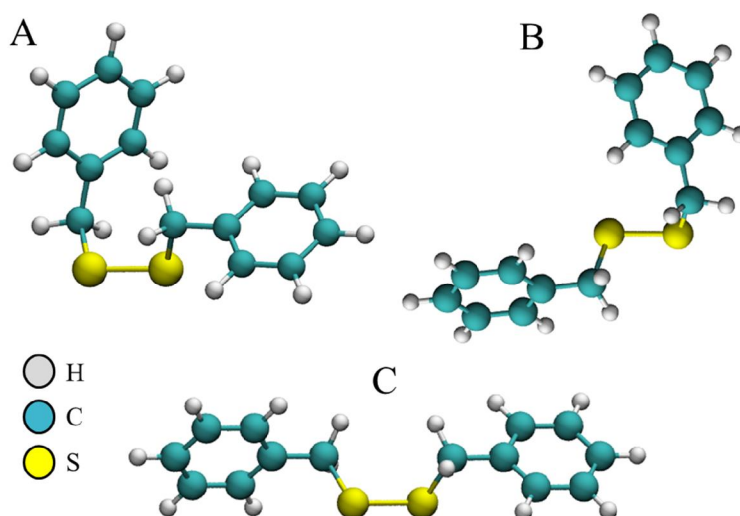

Fig 2. Schematic representation of the adsorption complex showing selected geometrical parameters used in the discussion of the adsorption site and geometry.
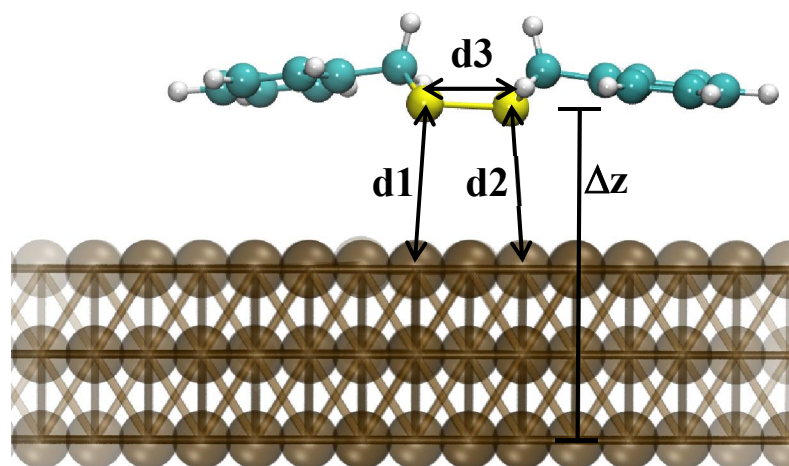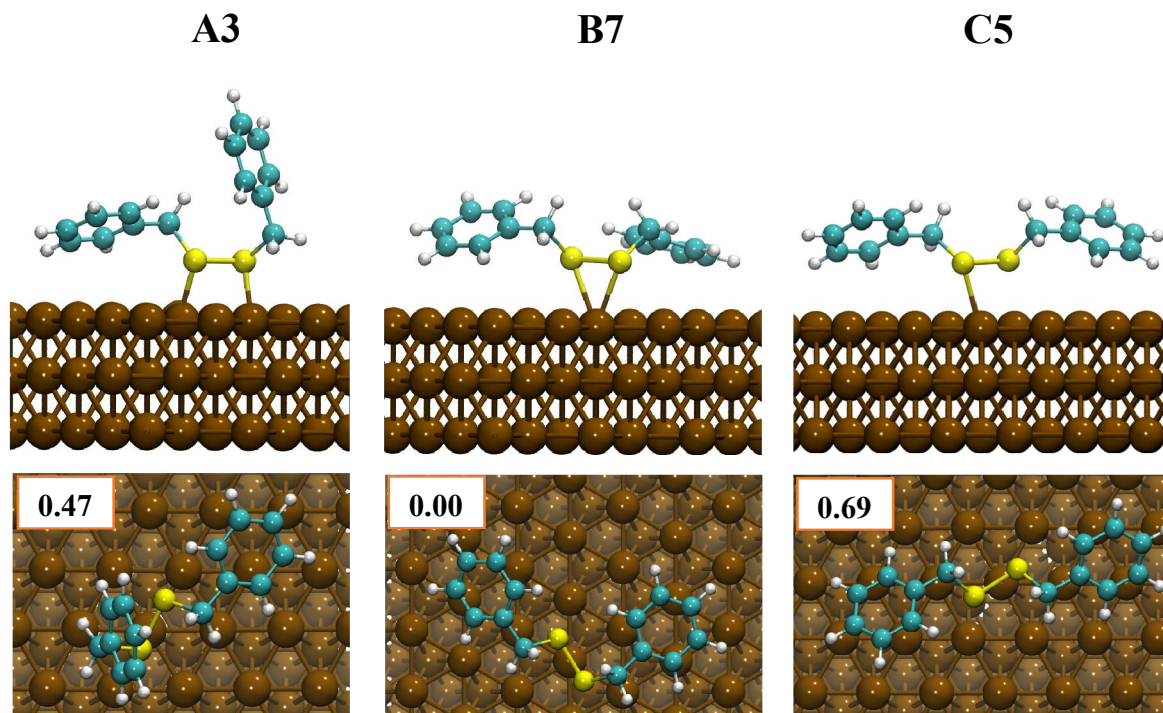
Fig 3. Some selected structures of physisorbed *DBDS* on Cu(111), showing their relative adsorption energy. (PBE-D2 energies in eV)

A3 **B7** **C5**

*In case of D2-1layer energies, the relative energies are 0.07, 0.00 y 0.25 eV, respectively.

Fig 4. Adsorption geometry of the most stable dissociated *DBDS* molecule on Cu(111) showing the distortion through Cu-Cu distances (in red) after adsorption.
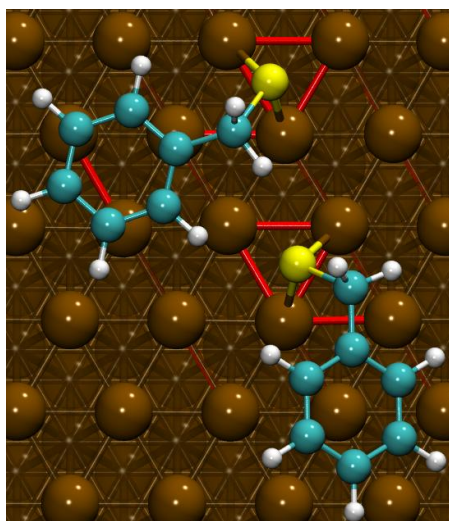
Fig 5. Top and side view of the most favorable adsorption geometry (B1) for *DBDS* on Cu(111).
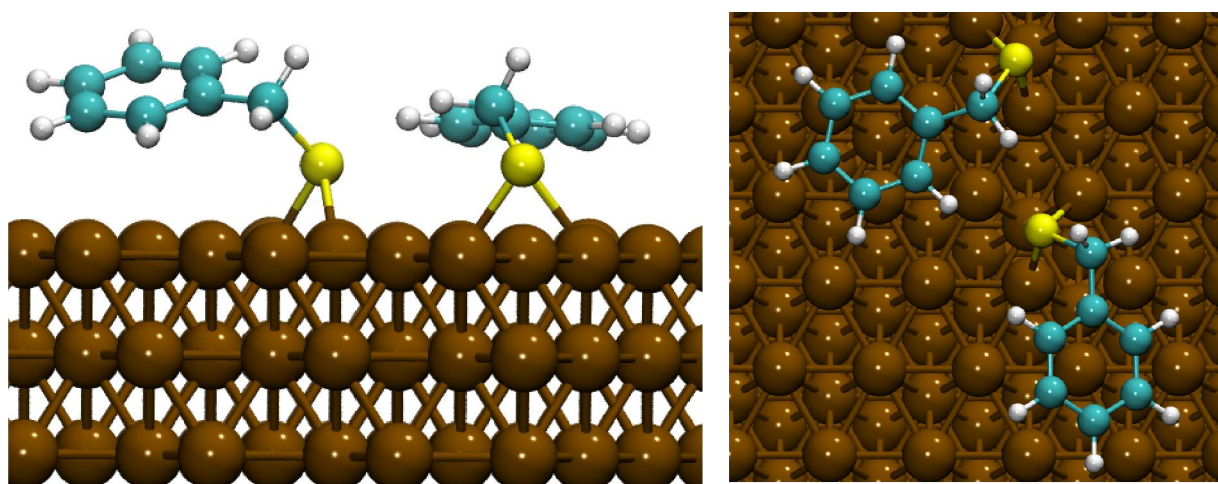
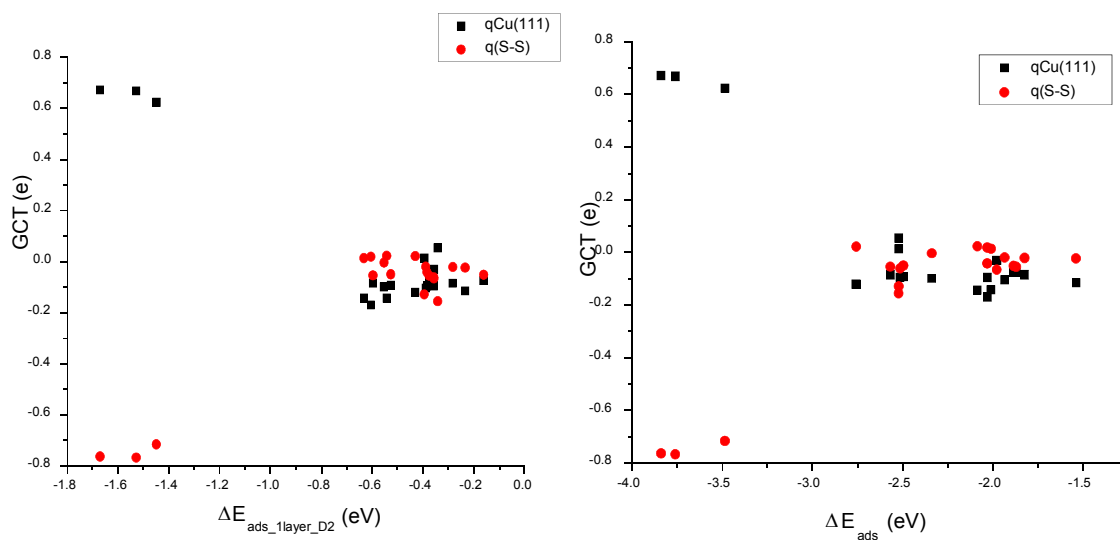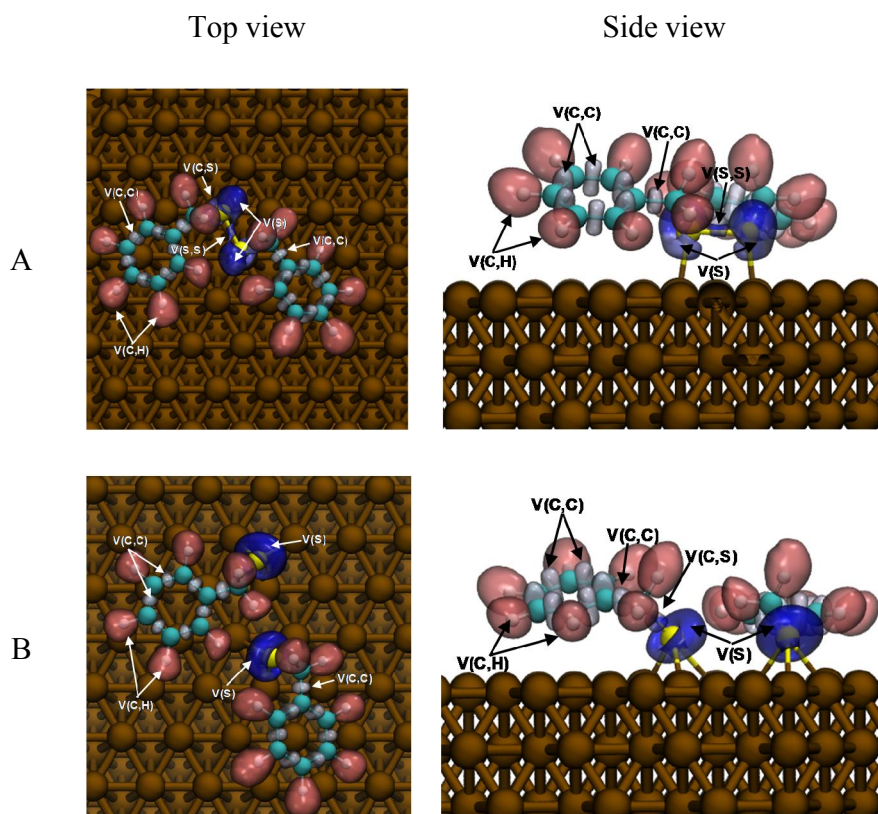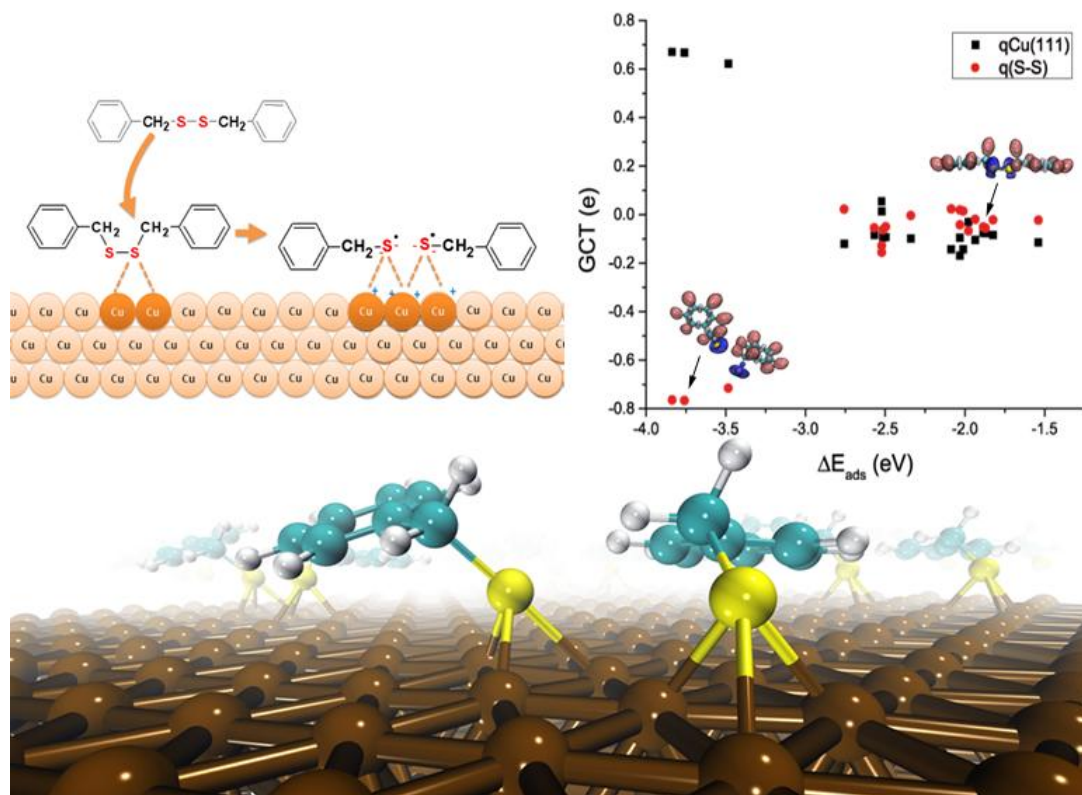**Fig 6.** General Charge transfer (GCT) vs adsorption energies (ΔE_{ads} and $\Delta E_{ads\_1layer\_D_2}$).

Fig 7. Selected ELF Isosurfaces (ELF=0.80) for (A) Physi- and (B) Chemi-sorption complexes formed by *DBDS* adsorption on copper surface

Top view   Side view

TOC?

TOC ?

DBDS adsorption on Cu(111):
Modelling the corrosion phenomenon

Cu²⁺

Cu₂S

SAM